ISSN 1330-3651 (Print), ISSN 1848-6339 (Online)
https://doi.org/10.17559/TV-20231221001225
Original scientific paper

Fuzzy Multi-Objective Structural Optimization Design of Reducer Housing for Oil Tea Fruit Shelling Machine

Di KANG, Longsheng CHEN, Shaofeng PENG, Wanyuan LI, Delin WU, Yang HAI, Chengji MI*

Abstract: In order to reduce the weight of the reducer housing and improve the structural performance of the housing, a fatigue-resistant lightweight design method in consideration of multi-source uncertainties was proposed. The numerical transient response analysis was utilized to analyze the dynamic characteristics of the cast iron reducer housing, and the simulation results were in good agreement with the experimental data. The stiffness fuzzy multi-objective topology optimization function was constructed with three static conditions and third-order dynamic frequencies based on the fuzzy variable weight coefficients, the fuzzy multi-objective topology optimization design was carried out on the reducer housing to obtain the new reducer housing. Then, the anti-fatigue and lightweight co-optimization design of the rebuilt reducer housing considering multi-sources uncertainties was performed. The optimized results showed that the weight was reduced by 13.2% while under the premise of ensuring the fatigue life.

Keywords: anti-fatigue and lightweight co-optimization; fuzzy variable weight coefficient; multi-objective optimization; multi-sources uncertainties

1 INTRODUCTION

As one of the important load-bearing components of the reducer, the reducer housing must meet the strength and stiffness requirements. The redundant design is utilized to meet the performance requirements of the traditional design method [1]. Topology optimization, based on mathematical models and optimization algorithms, is used to search for the best topology within a given design domain [2]. Some researchers have carried out some work to optimize reducer. A single objective optimization model of the reducer is established, which includes six design variables and takes the minimum mass of the reducer as the objective function [3]. A method for optimizing the motor is presented, with the objectives of minimizing its weight and maximizing its efficiency [4], while the above studies mainly focus on the deterministic design optimization (DDO) of the reducer. However, they ignore the fact that the design parameters may be affected by uncertainties such as manufacturing deviations, assembly errors, changes in workloads, etc. The feasibility and reliability of the optimization results are difficult to ensure.

Many researchers have considered uncertainty in structural optimization. A fuzzy satisfaction variable weighting coefficients are constructed to dynamically assign each single objective weighting coefficient for topology optimization of the pallet [5]. A multi-objective reliability optimization method for door design is proposed using a probabilistic model [6]. A reliability-based design optimization method is proposed to enhance the crash worthiness of foam-filled asphalt conical structures by considering the uncertainties of design variables and noise factors [7]. An application of fuzzy set theory and sequential multilevel approach is utilized for multi-objective topology optimization problems of continuum structures [8]. A fuzzy set model-based multi-objective topology optimization method for reliability is proposed, which considers the uncertainties of the structural parameters [9]. All these optimization methods for uncertainty are based on probabilistic models. Unfortunately, a large amount of uncertainty information is needed to construct the exact probability distribution of the uncertain values, which is very expensive.

The biggest advantage of interval analysis compared to probabilistic and fuzzy analysis in uncertainty problems is that it requires fewer samples and is simpler to express uncertain information. A method for multi-objective design, based on the satisfaction function, is proposed to solve the problem of multi-objective optimal design for a rotating guard rail with uncertain sectional parameters [10]. An interval robust optimization method is proposed using uncertainty structures as the object of study [11]. An interval uncertainty optimization model considering robustness is developed using the interval order method and the interval probability degree method [12]. An equivalent deterministic approach is proposed for design optimization models based on interval uncertainty [13].

In this paper, the dynamic characteristics of the reducer housing are investigated by finite element simulation and compared with the experimental results. Then, a multi-objective topology optimization function is constructed by introducing variable weight coefficients based on fuzzy theory, and new housing is obtained by fuzzy multi-objective topology optimization design of the reducer housing. Finally, considering the multi-source uncertainty, the modified reducer housing is designed with anti-fatigue and lightweight co-optimization.

2 METHODS AND EXPERIMENTAL

2.1 Boundary Conditions

The dynamic excitation force is applied to the reducer housing through the bearing bore. The reducer housing is subjected to the distributed radial reaction force F_R at the bearing hole position [14] as shown in Fig. 1.

The bearing bore is subjected to both a combined radial force F_R and an axial force F_a. The expression for the combined radial force F_R is given below:

$$F_{Ri} = \sqrt{{F_{ri}}^2 + {F_{ti}}^2} \tag{1}$$

where F_{Ri} denotes the radial combined force on the bearing bore for i-th. F_{ri} shows the radial force on the i-th bearing hole, and F_{ti} indicates the circumferential force on the i-th bearing hole.

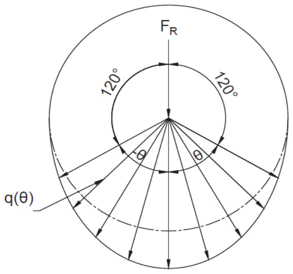

Figure 1 Diagram of radial resultant force distribution in the bearing bore

Table 1 Force at shaft support under positive rotation condition

Components	Force / N	Components	Force / N
F_{r1}	79,75	F_{t1}	30,57
F_{r2}	79,75	F_{t2}	30,57
F_{r3}	79,75	F_{t3}	219,1
F_{r4}	79,75	F_{t4}	219,1

When the reducer works normally at the rated speed of 1455 r/min, the force at each shaft support position is shown in Tab. 1. Among them, F_{i1} and F_{i2} are the forces at the input shaft support position, and F_{i3} and F_{i4} are the forces at the output shaft support position. Then the distributed pressure $q(\theta)$ could be considered as [15]:

$$q\left(\theta\right)=\frac{5F_R}{6RL}\cos\left(\frac{3}{2}\theta\right) \tag{2}$$

where F_R is the radial force on the bearing bore, R is the radius of the bearing bore, L is the width of the bearing bore, θ is the angle, and the specific angle B is equal to 120°.

2.2 Finite Element Model

In order to study and optimize the static and dynamic characteristics of the reducer housing the SolidWorks [16] model file can be directly imported into the HyperMesh software [17]. The chamfers and technology holes in the real structure are simplified, as shown in Fig. 2.

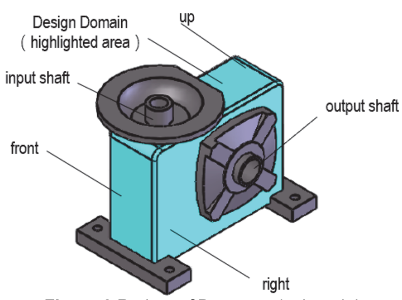

Figure 2 Reducer 3D geometrical model

The overall size of the mesh was controlled within 6 mm to ensure the accuracy and computational efficiency of the model. Finally, the model consists of 57082 hexahedral cells and 72820 nodes, as shown in Fig. 3. The material of the reducer housing is selected as HT200.

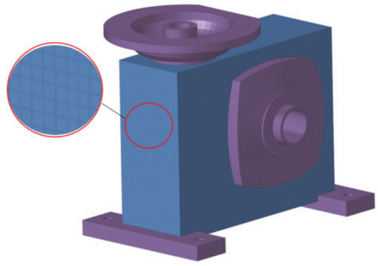

Figure 3 Reducer finite element model

2.3 Dynamic Response Tests

In order to analyze the dynamic characteristics of reducer housing, the test bench is established as shown in Fig. 4. The accelerometer used in this experiment is a small, high-range, high-frequency piezoelectric EGAXT-50-C20104 accelerometer with a sensitivity of approximately 2.439 mV/g, which is used to collect the vibration acceleration response at critical points of the reducer housing, as shown in Fig. 5. The Kenkyujo data collector, a small multi-channel data acquisition instrument that can simultaneously measure a combination of sensors with a sampling frequency of up to 100 kHz, was used for testing conditions at a rated motor speed of 1455 r/min and an input torque of 50Nm. The acceleration sensor was tested with a sampling frequency of 100 Hz for 10 seconds. The test results were obtained by collecting the vibration response of the test points, as shown in Fig. 6.

Figure 4 Test bench

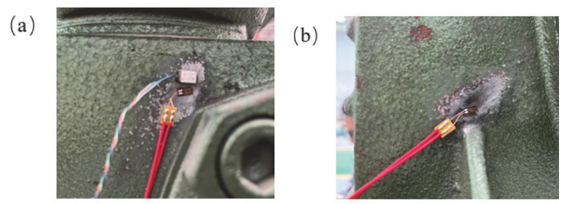

Figure 5 Acceleration measuring positions of reducer; (a) Input shaft measurement point position; (b) Output shaft measurement point position

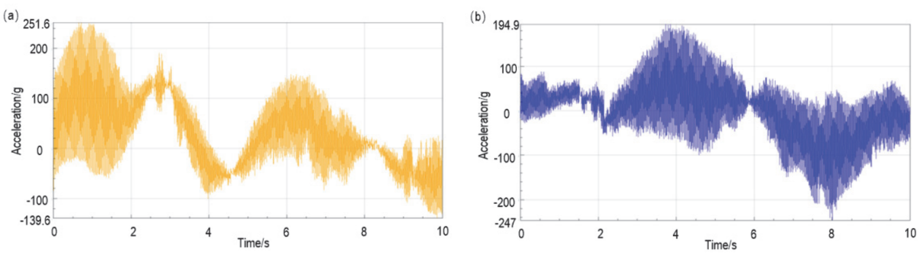

Figure 6 Acceleration history at two measurement points; (a) Input shaft position; (b) Output shaft position

2.4 Transient Response Simulation

In the dynamic frequency simulation, the measured acceleration time signal is used as the transient excitation of the input shaft position of the reducer, and the simulation parameters are consistent with the test parameters. The acceleration sensor is placed at the output shaft position to obtain the acceleration time signal at the output shaft position, as shown in Fig. 7.

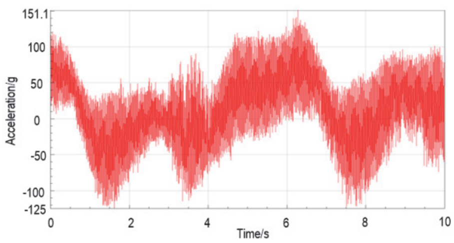

Figure 7 Transient acceleration at output shaft

Finally, the acceleration time signal in the time domain is converted to the acceleration power spectral density in the frequency domain, and the results are shown in Fig. 8. The first six orders of the intrinsic frequency data between the experimental data and the simulation results are obtained with a good agreement. The results are represented in Tab. 2.

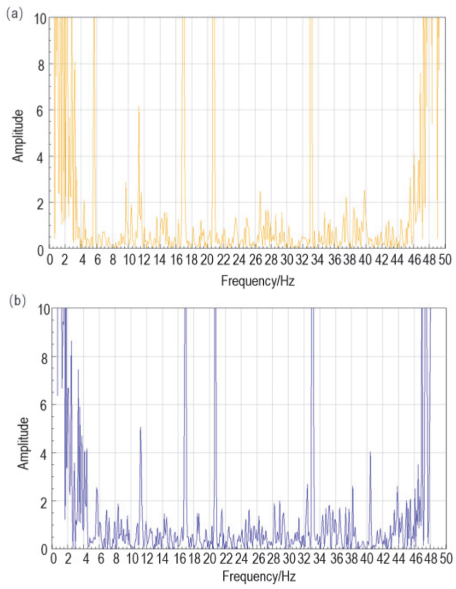

Figure 8 Comparison of experimental and simulated acceleration power spectral density at the output shaft of reducer; (a) Tested data; (b) Simulated results

Table 2 Comparison of dynamic frequency experimental data and finite element data (Hz)

	Test data	Simulated data
1st order	3,30	3,21
2nd order	11,30	11,25
3rd order	16,81	16,77
4th order	20,99	20,68
5th order	33,19	33,19
6th order	40,47	39,85

3 RESULTS AND DISCUSSION

3.1 Theory of Optimal Design of Structural Topology

Structural topology optimization is the search for the best material distribution solution for objects subjected to single or multiple loads. This optimization approach is expressed in optimal design as a "minimum flexibility (maximum stiffness)" design. There are three main types of structural topology optimization methods: the Homogenization method, the ESO method, and the Variable Density Method. In this paper, the variable density method is adopted, and its mathematical model is briefly described below. Structural topology optimization is to detect a sub-region Ω_{mat} (concerning the material region) of a given volume $\overline{V}$ within a design region Ω and make the optimization objective function θ corresponding to this design region obtain an extreme value. $\forall x \in \Omega$ It is assumed that the density function of the material is expressed as [18].

$$\rho(x)=\begin{cases}0, & \left(x \in \Omega^{mat}\right) \\ 1, & \left(x \in \Omega / \Omega^{mat}\right)\end{cases} \tag{3}$$

So the mathematical model for topology optimization can be represented as:

$$\min_{\rho} \ \phi(\rho) \tag{4}$$

$$s.t. \quad \int_{\Omega} p d\Omega \leq \overline{V} \tag{5}$$

$$\rho(x)=0 \text{ or } 1(\forall x \in \Omega) \tag{6}$$

Using the finite element ideology, the design domain of the structure Ω is divided into n cells, while the corresponding density function ρ is approximated as ann-dimensional vector $\boldsymbol{X}=(\boldsymbol{X_1}, \boldsymbol{X_2}, \ldots, \boldsymbol{X_n})$, where X_i is the density value corresponding to each cell i. The design domain of the structure is discretized into cells. Then the optimization model is transformed into an integer mathematical optimization model represented by 0 and 1:

$$\min_{X} \ \phi(X) \tag{7}$$

$$s.t. \quad V(x)=\sum_{i=1}^{n} \rho_i v_i \leq \overline{V} \tag{8}$$

$$\rho_i=0 \text{ or } 1 \quad i=(1, 2, 3, \ldots, n) \tag{9}$$

limited to the integer type Mathematical models are computationally difficult to solve. The problem is solved by making the variables continuous, transforming the 0 and 1 integer variable optimization problem into a continuous variable optimization model in the interval [0, 1]:

$$\min_{X} \quad \phi(X) \tag{10}$$

$$s.t. \quad V(x)=\sum_{i=1}^{n} \rho_i v_i \leq \overline{V} \tag{11}$$

$$0<\delta<\rho_i\leq 1 \quad i=(1,\ 2,\ 3,\ ...,\ n) \tag{12}$$

In the above Eq. (12), δ takes an extremely small positive number for example (10^{-4}) to avoid singularities in the stiffness matrix. When the model after continuous variation of the above variables is a pathological problem, the optimized solution exhibits intermediate density values with checkerboard phenomenon and numerical instability. The above problems can be solved effectively by using checkerboard control measures and intermediate density penalty models. The commonly used density interpolation models are the SIMP model and RAMP model, and the SIMP material model is used in this paper. Its elastic modulus and density can be denoted as:

$$E_{ijkl}(x)=\rho(x)^p E_{ijkl}^0 \tag{13}$$

$$s.t. \quad \int_{\Omega}\rho(x)\mathrm{d}\Omega\leq V \tag{14}$$

where V is the allowable amount of material; the penalty factor, based on engineering experience $p\geq 3$ is optimized to be closer to the black-white form; the density function of the material $0\leq\rho(x)\leq 1$; and the design variable $x\in\Omega$.

3.2 Fuzzy Variable Weight Coefficient Method

In this paper, the objective function optimization result ambiguity is characterized by the introduction of the affiliation function and combined with the weighting coefficients in multi-objective optimization. The mathematical expression is [19].

$$\lambda_i=u_{f_i}(x)= \\ =\begin{cases} 1 & \left(f_i(x)\leq f_i^{\min}\right) \\ \dfrac{1}{1+\exp\left(a_1-a_2\dfrac{f_i(x)-f_i^{\max}}{f_i^{\min}-f_i^{\max}}\right)} & \left(f_i^{\min}<f_i(x)<f_i^{\max}\right) \\ 0 & \left(f_i(x)\geq f_i^{\max}\right) \end{cases} \\ (i=1,\ 2,\ \dots,\ n) \tag{15}$$

Among them, a_1, a_2 is a setting parameter used to regulate the trend of the affiliation function. a_1 takes the value of 2, a_2 takes the value of 4, $f_i^{\min}$ and $f_i^{\max}$ are the optimal value and the worst value of the single-objective, which corresponds to the minimum and maximum values of the strain energy in the single-objective stiffness topology optimization and the minimum and maximum values of the natural frequency in the single-objective intrinsic frequency optimization.

In the multi-objective topology optimization of speed reducer, there is ambiguity between single objectives of multiple working conditions and the weight coefficients of sub-objectives are dynamically assigned by the fuzzy variable weight coefficient method. The mathematical expressions of fuzzy variable weight coefficients w_i and w_j are [19, 20]:

$$w_i=\frac{1-\lambda_i}{\sum_{i=1}^{n}(1-\lambda_i)} \tag{16}$$

$$w_j=\frac{1-\lambda_j}{\sum_{j=1}^{n}(1-\lambda_j)} \tag{17}$$

3.3 Fuzzy Multi-Objective Topology Optimization Mathematical Function

According to the compromise planning method, the static stiffness under three working conditions of the reducer housing and the first three orders of the inherent frequency of the reducer are taken as the optimization objective. The volume fraction and fatigue stress are taken as the constraints, so as to establish the static-dynamic multi-objective topological optimization mathematical model of the reducer housing as shown in the following equations:

$$\min\Phi(\rho)=\left\{\begin{matrix} a^2\sum_{i=1}^{n}\left[w_i\dfrac{C_i(\rho)-C_i^{\min}}{C_i^{\max}-C_i^{\min}}\right]^2+ \\ (1-a)^2\sum_{j=1}^{n}\left[w_j\dfrac{\psi_{j\max}-\psi_j(\rho)}{\psi_{j\max}-\psi_{j\min}}\right]^2 \end{matrix}\right\}^{\frac{1}{2}} \tag{18}$$

where is the total number of loading conditions, w_i is the weight factor of the i-th condition, $C_i(\rho)$ is the strain energy objective function of the i-th condition, $C_{\mathrm{i}}^{\max}$ and $C_{\mathrm{i}}^{\min}$ are the maximum and minimum values of the strain energy of the i-th condition. $\psi_j(\rho)$ is the j-th order intrinsic frequency objective function, ψ_{jmax} and ψ_{jmin} are the maximum and minimum values of the j-th order frequency optimization of the reducer under the free vibration condition; a is the weight of the strain energy objective in the multi-objective optimization, $1-a$ is the weight of the intrinsic frequency objective in the multi-objective optimization, and in this paper, a is taken as 0,5.

3.4 Topology Optimization Parameter Settings

The process of optimal design is to find the design variables that satisfy the constraint function to make the objective function optimal, therefore, the elements need to be determined. The density of each unit in the blue area of the design domain shown in Fig. 3 is used as the design variable; the upper limit of the constraint of the volume ratio is set to 0,4 as the constraint function; and the maximum stiffness of the forward, reverse and start-up conditions and the maximum frequency of the first three orders are used as the objective function.

In addition, topology optimization-related parameters also have a greater impact on the optimization results in the optimization process. Some important parameters are set as follows: DESMAX means that the maximum number of optimization iterations is set to 80; the discretization parameter is set as DISCRETE 3.0; the CHECKER tab of the checkerboard control parameter is set to 1. In addition, to meet the demand of manufacturing, the left-right face symmetry constraint and the left-right face extraction constraint can be added to make the result easier to manufacture.

3.5 Topology Optimization Results

After setting the optimization parameters, the final fuzzy multi-objective topology optimization structure of the reducer housing is obtained after 71 iterations, as shown in Fig. 9, which is submitted to OptiStruct for calculation. A "herringbone" reinforcement structure is present on the front side of the reducer housing, with transverse reinforcements on the left, right, and rear sides, which are symmetrically distributed due to symmetrical constraints. This structure improves the housing stiffness and inherent frequency and reduces the stress level at the connection between the housing and the bottom mounting position. Detailed information is shown in Tab. 3. The maximum deformation under each working condition was reduced by 28.6%, −4.5%, and 14.1%, and the third-order frequency under the constrained modes was increased by 13.2%, 11.3%, and 33.1%, respectively. According to the optimized geometry, the modified reducer housing is shown in Fig. 10. The optimized reducer housing structure can be used as a reference basis for further lightweight design of the reducer housing.

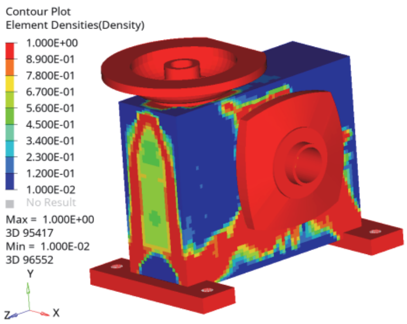

Figure 9 Fuzzy multi-objectives topology optimization structure of reducer housing

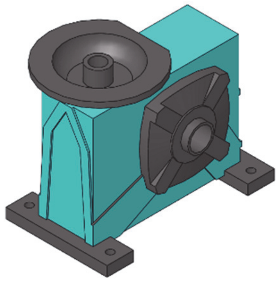

Figure 10 Structure diagram of the new reducer housing

Table 3 Comparison of initial and optimized reducer housing

	Initial	Optimized	Variation
Df_{max} / ×10^{-4}mm	9,774	6,979	−28,60%
Dr_{max} / ×10^{-4} mm	7,034	7,354	4,50%
Ds_{max} / ×10^{-4} mm	11,271	9,679	−14,10%
Fr_1 / Hz	262,2	302,1	13,20%
Fr_1 / Hz	561	632,5	11,30%
Fr_1 / Hz	591,3	883,4	33,10%

4 ANTI-FATIGUE AND LIGHTWEIGHT CO-OPTIMIZATION DESIGN

4.1 Optimization Method

In general, the material properties of reducer housing in the manufacturing period are uncertain because of process inconsistency, as well as geometrical structure size. In order to fully take uncertain factors into account, the interval multi-objectives optimization function could be described as [21, 22].

$$\begin{cases} \min\ f_i(X,U) \\ s.t.:\ g_i(X,U) \le b_i^I = \left[b_i^L, b_i^R\right] \\ i = 1, 2, ..., l;\ X \in \Omega^n \\ U \in U^I = \left[U^L, U^R\right], U_i \in U_i^I = \left[U_i^L, U_i^R\right] \\ i = 1, 2, ..., q \end{cases} \tag{19}$$

where $f_i(X,U)$ and $g_i(X,U)$ denote the objective function and the constraint function, respectively; X is an n-dimensional design variable with the value range Ω^n; U is a q-dimensional uncertainty variable, and its uncertainty is described by a q-dimensional interval vector U^I, where L and R are the lower and upper bounds of the interval; b_i denotes the permissible interval for the i-th uncertainty constraint, which is a continuous function of U within the interval.

Then, the interval uncertain optimization function can be transformed into an interval certain optimization function, and is rewritten as [21-24]:

$$\begin{cases} \min(f^c(X), f^w(X)) \\ f^c(X) = \dfrac{\min(f(X,U)) + \max(f(X,U))}{2} \\ f^w(X) = \dfrac{\max(f(X,U)) - \min(f(X,U))}{2} \end{cases} \tag{20}$$

where $f^c(X)$ and $f^w(X)$ is the interval midpoint value and radius value of the objective function. Further, the interval multi-objectives poetization function could be transformed into an interval single-objective optimization function, and is rewritten as [21-24]:

$$\min f(X) = \alpha f^c(X) + (1-\alpha) f^w(X) \tag{21}$$

where α is weight coefficient within $0 \le \alpha \le 1$, and is considered as 0,5 in this paper.

4.2 Determination of Optimization Function

In order to conduct the anti-fatigue and lightweight co-optimization design, the weight and minimum fatigue life of topology-optimized reducer housing are considered as the optimization objectives. The width and thickness of four reinforcing ribs are treated as design variables. The modulus of elasticity, Poisson's ratio, and density are taken as the uncertain factors. Then, the optimization function can be described as [25]:

$$\begin{aligned} &\max N(x_1, x_2, x_3, x_4) \\ &\min W(x_1, x_2, x_3, x_4) \\ &s.t. xi \in Xi, i = 1,2,3,4 \end{aligned} \tag{22}$$

where $N(x_1, x_2, x_3, x_4)$ and $W(x_1, x_2, x_3, x_4)$ are fatigue life optimization objective and weight optimization objective, respectively. x_1, x_2, x_3 and x_4 are the thickness of the cross-beam in the upper-end cover, the width of the cross-beam in the upper-end cover, the width of the longitudinal stiffening rib in the upper-end cover, and the width of the cross-beam in the lower-end cover.

Based on the Latin hypercube sampling method, five sets of uncertain variables are listed in Tab. 4.

Table 4 Sample data of uncertainty quantity

	E / GPa	μ	ρ / 103 Kg/m^3
No.1	107	0,26	7,2
No.2	110	0,25	7,7
No.3	114	0,29	7,1
No.4	115	0,27	7,1
No.5	119	0,28	7,7

The 20 sets of design variables are shown in Tab. 5, and the corresponding fatigue life response values and weight response values are shown in Fig. 6. By 5 groups of uncertainty variables with 20 groups of design variable samples, 100 groups of sample values are obtained. These 100 sets of data are used to operate the finite element model, and the corresponding fatigue life response and weight response values of the reducer housing can be derived.

Table 5 Design variables data

No.	x_1 / mm	x_2 / mm	x_3 / mm	x_4 / mm
1	2,0	3,9	13,0	5,2
2	2,2	5,2	13,6	2,6
3	2,4	5,0	11,7	3,7
4	2,6	3,1	11,1	2,2
5	2,8	5,4	8,5	4,1
6	3,1	6,0	15,5	2,4
7	3,3	3,7	14,8	5,0
8	3,5	4,5	10,4	4,5
9	3,7	3,5	17,4	3,3
10	3,9	5,6	6,0	3,9
11	4,1	2,4	7,3	3,5
12	4,3	4,3	9,2	5,6
13	4,5	4,1	12,3	5,8
14	4,7	5,8	16,7	4,3
15	5,0	3,3	6,6	2,0
16	5,2	2,2	14,2	4,7
17	5,4	2,6	16,1	5,4
18	5,6	4,7	9,8	2,8
19	5,8	2,0	18,0	3,1
20	6,0	2,8	7,9	6,0

Concerning Eq. (20) and Eq. (21), combined with the data in Tab. 5, the uncertainty problem is transformed into a deterministic problem solving, and the corresponding optimization objective function of fatigue life and weight of the reducer housing is established, whose mathematical expression is shown in Eq. (23) and Eq. (24) [21-24].

$$\begin{cases} \max N(X) = \alpha N^c(X) + (1-\alpha) N^w(X) \\ N^c(X) = \dfrac{\min(N(X,U)) + \max(N(X,U))}{2} \\ N^w(X) = \dfrac{\max(N(X,U)) - \min(N(X,U))}{2} \end{cases} \tag{23}$$

$$\begin{cases} \min W(X) = \alpha W^c(X) + (1-\alpha) W^w(X) \\ W^c(X) = \dfrac{\min(W(X,U)) + \max(W(X,U))}{2} \\ W^w(X) = \dfrac{\max(W(X,U)) - \min(W(X,U))}{2} \end{cases} \tag{24}$$

Table 6 Response values

No.	Nf_{min}/×107cycle	Nf_{max}/×107cycle	W_{min}/ kg	W_{max}/ kg
1	1,3	1,6	43,8	44,9
2	1,6	2,0	42,8	44,9
3	1,6	1,9	42,8	44,9
4	1,2	1,5	42,6	44,7
5	1,7	2,1	43,0	45,1
6	2,0	2,5	43,0	45,1
7	1,3	1,6	43,0	45,1
8	1,5	1,8	43,0	45,1
9	1,3	1,6	42,9	45,0
10	1,8	2,3	43,1	45,2
11	1,2	1,4	42,8	44,9
12	1,5	1,8	43,2	45,3
13	1,4	1,8	43,2	45,3
14	2,0	2,5	43,3	45,5
15	1,3	1,6	42,9	45,0
16	1,2	1,5	43,1	45,2
17	1,2	1,6	43,2	45,3
18	1,6	2,0	43,2	45,3
19	1,2	1,5	43,0	45,2
20	1,3	1,6	43,3	45,4

Then the approximate model of the design variables and the two optimization objective functions max $N(x)$ and min $W(x)$ is established by the second-order response surface method with the following mathematical expressions:

$$\begin{aligned} N(x) &= 1,05 - 3,6\times10^{-2}\cdot x_1 - 1,77\times10^{-1}\cdot x_2 - \\ &-1,32\times10^{-2}\cdot x_3 - 1,3\times10^{-2}\cdot x_4 + 3,6\times10^{-3}\cdot \\ &\cdot x_1^2 + 3,59\times10^{-2}\cdot x_2^2 + 4,29\times10^{-4}\cdot x_3^2 + \\ &+3,57\times10^{-3}\cdot x_4^2 + 5,91\times10^{-3}\cdot x_1\cdot x_2 + 1,55\times \\ &\times10^{-4}\cdot x_1\cdot x_3 - 4,26\times10^{-4}\cdot x_1\cdot x_4 + 8,9\times \\ &\times10^{-4}\cdot x_2\cdot x_3 - 3,13\times10^{-3}\cdot x_2\cdot x_4 + 2,14^{-4}\cdot \\ &\cdot x_3\cdot x_4 \end{aligned} \tag{25}$$

$$\begin{aligned} W(x) &= 21,9 + 6,41\times10^{-2}\cdot x_1 + 2,38\times10^{-2}\cdot x_2 + \\ &+1,92\times10^{-3}\cdot x_3 + 2,96\times10^{-2}\cdot x_4 - 8,34\times10^{-4}\cdot \\ &\cdot x_1^2 + 2,28\times10^{-3}\cdot x_2^2 + 1,28\times10^{-4}\cdot x_3^2 + 3,3\times \\ &\times10^{-3}\cdot x_4^2 + 3,92\times10^{-3}\cdot x_1\cdot x_2 + 2,98\times10^{-4}\cdot \\ &\cdot x_1\cdot x_3 - 1,64\times10^{-3}\cdot x_1\cdot x_4 - 2,36\times10^{-4}\cdot x_2\cdot \\ &\cdot x_3 - 2,4\times10^{-3}\cdot x_2\cdot x_4 - 4,62\times10^{-4}\cdot x_3\cdot x_4 \end{aligned} \tag{26}$$

where $N(x)$ is the fitted fatigue life objective function response value of the reducer housing; $W(x)$ is the fitted weight objective function response value of the reducer housing, and x_1, x_2, x_3, x_4 is described in the previous section.

In Fig. 11, the main effect relationship between the design variables and the fatigue life objective function response of the reducer housing is demonstrated. Based on the results presented in the figure, all four variables (x_1, x_2,

x_3, x_4) have a positive effect on the value of the fatigue life objective function response of the reducer housing. In particular, the slope of the contribution factor increases gradually and has the highest impact.

In Fig. 12, the main effect relationship between the design variables and the reducer case weight objective function response is demonstrated. The four variables (x_1, x_2, x_3, x_4) also have a positive effect on the value of the reducer case weight objective function response. Among them, the contribution factor of x_1 has the highest impact.

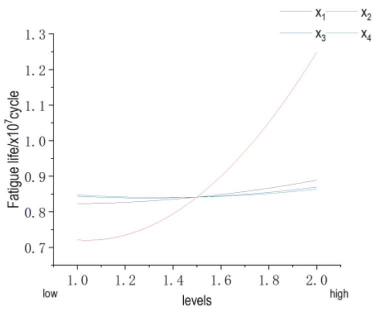

Figure 11 Main effect diagram of design variables and fatigue life objective of reducer housing

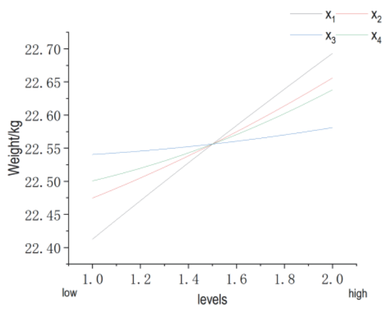

Figure 12 Main effect diagram of design variables and reducer housing weight objective

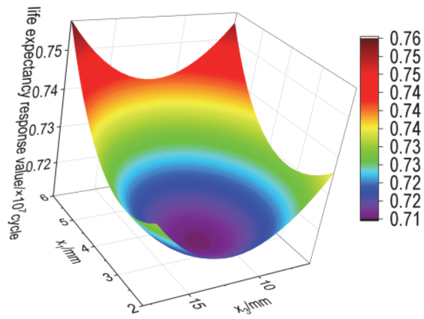

Figure 13 Relationship between design variables x_1 and x_3 and fatigue life objective function values

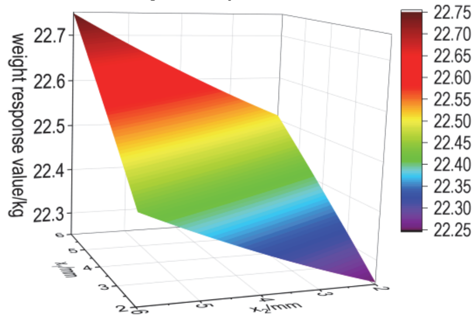

Figure 14 Relationship between design variables x_1, x_2 and weight objective function values

Fig. 13 shows the relationship between some of the design variables and the fatigue life objective function response values of the reducer housing. There is a clear non-linear relationship between the design variables x_1, x_3 and the fatigue life objective function response value of the reducer housing. Especially for the variables x_1 and x_3, their effects on the fatigue life objective function response values are more significant than the other variables. In addition, the effect of the variable x_1 on the fatigue life objective response value is significantly greater than that of the variable x_3.

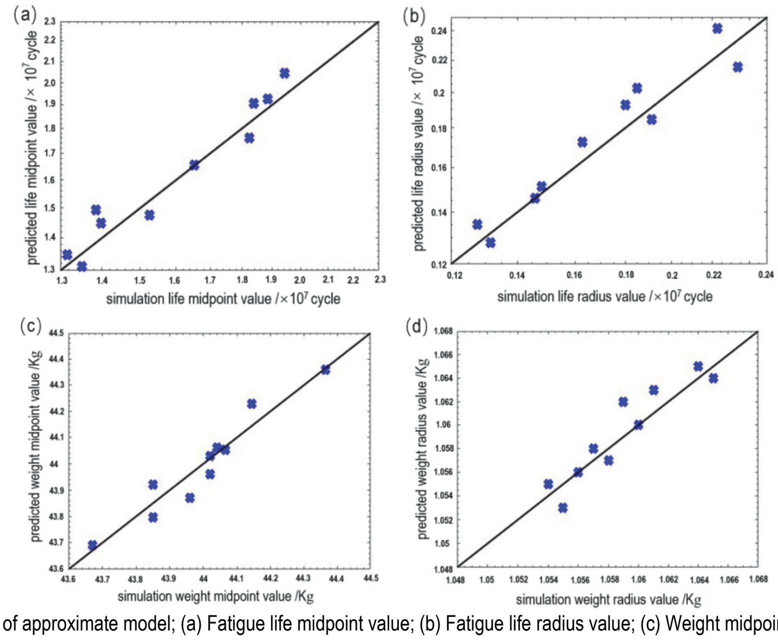

Figure 15 Accuracy validation of approximate model; (a) Fatigue life midpoint value; (b) Fatigue life radius value; (c) Weight midpoint value; (d) Weight radius value

Similarly, a similar non-linear relationship can be observed based on the relationship between some of the design variables and the response values of the reducer case weight objective function presented in Fig. 14. Among them, the effects of x_1 and x_2 on the reducer case weight objective function are more significant. The variable x_1 has a greater effect on the reducer case weight objective response value than the variable x_2.

To verify the accuracy of the established approximation model, ten sample points within the total design variable space that were not sampled by the Latin hypercube sampling were selected and substituted into the finite element model for analysis and the approximation model for prediction, respectively, and the data of the two were compared, and the results of the validation are displayed in Fig. 15.

4.3 Results of Interval Multi-Objectives Optimization

In this paper, a Non-dominated Sorting Genetic Algorithm with Elite Strategy (NSGA-II) is used for optimal design. Using insight software, the number of populations is set to 20, the number of iterations is 100, and the weights of the two objective functions of fatigue life and the weight of the reducer housing are both set to 0,5. Then, the optimal result is obtained, as listed in Tab. 7.

Table 7 Design variables and maximum and minimum optimized objective response values

	Initial	Optimized	Variation
x_1 / mm	4,0	2,0	−2,0
x_2 / mm	4,0	6,0	1,2
x_3 /mm	12,0	6,0	−6,0
x_4 /mm	4,0	2,0	−2,0
Fatigue life / × 10^7 cycle	1,13	1,44	0,31
Weight / kg	49,46	42,92	−6,54

As we can see from Tab. 7, except for x_2 , the design variables x_1, x_3, x_4 are reduced from the original values and the amplitude change of all the variables reaches about 50%. The fatigue life of the reducer housing is slightly increased. At the same time, the weight of the reducer housing has been reduced by 6.54 kg (13.2%) which meets the design requirement.

5 CONCLUSIONS

An anti-fatigue and lightweight design method for reducer housings that takes uncertainties into account is proposed through static and dynamic analyses of the reducer housings. The method takes into account the material properties and the uncertainties that may exist in the processing and manufacturing process, and by combining finite element analysis with topology optimization and size optimization techniques, a reducer housing structure with high strength and lightweight characteristics is obtained. The details are as follows:

(1) The reducer housing is modeled by solid elements and transient response analysis is carried out. The first-order frequency of simulated result is 3.21 Hz, which was in good agreement with the experimental data.

(2) A fuzzy multi-objective topology optimization model of the reducer housing is established based on the fuzzy variable weight coefficient method, and the optimized reducer housing is reconstructed according to the iterative results. The optimized results show that $Dr_{\max}$ is increased by 4.5%, and the first to three-order frequency is increased by 13.2%, 11.3% and 33.11%, respectively. However, $Df_{\max}$ and $Ds_{\max}$ are decreased by 28.6% and 14.1%, respectively.

(3) A collaborative optimization design study of anti-fatigue and lightweight of the reducer housing is carried out based on the genetic algorithm, while the fatigue life is increased by 27.4% and the weight is reduced by 13.2%. This suggested method may be helpful for the optimization design of engineering structure, especially in mechanical parts.

Nomenclature

$Df_{\max}$ - Maximum deformation of the reducer housing under positive rotation conditions
$Dr_{\max}$ - Maximum deformation of the reducer housing under reversing conditions
$Ds_{\max}$ - Maximum deformation of the reducer housing under starting conditions
Fr_1 - 1st order intrinsic frequency
Fr_2 - 2nd order intrinsic frequency
Fr_3 - 3rd order intrinsic frequency
E - Elastic modulus (GPa)
μ - Poisson's ratio
ρ - Density
$Nf_{\min}$ - Minimum uncertain fatigue life
$Nf_{\max}$ - Maximum uncertain fatigue life
$W_{\min}$ - Minimum uncertain weight
$W_{\max}$ - Maximum uncertain weight

Acknowledgements

This paper is supported by State Forestry and Grassland Administration Emergency Science and Technology Project (Grant No.:202202-8); Forestry Science and Technology Innovation Project of Hunan Province (Grant No: XLK201910); Technology Innovation Entrepreneurial Team of Hunan Shennong National Oil Tea Industry. It is supported by the Central Forestry Finance Science Technology Promotion and Demonstration Fund Project (Grant No. [2023] XT21) and the Hunan Oil Tea Industry Research Demonstration Project.

6 REFERENCES

[1] Zhu, J. L. (2023). *Modular energy-saving design of bridge crane trolley for green service*. Taiyuan University of Science and Technology.
[2] Gao, J., Xiao, M., Zhang, Y., & Gao, L. (2020). A comprehensive review of isogeometric topology optimization: methods, applications and prospects. *Chinese Journal of Mechanical Engineering, 33*(1), 1-14. https://doi.org/10.1186/s10033-020-00503-w
[3] Han, L. S., Hao, H., & Dong,Y. F. (2021). The Optimal Design of the 2K-V-type Cycloid-pin Reducer on the Modern Design Method. *Third International Conference on Digital Manufacturing & Automation*, *2012*, 927-930, https://doi.org/10.1109/ICDMA.2012.219
[4] Msaddek, H., Mansouri, A., & Trabelsi, H. (2023). Optimal Design and Cogging Torque Minimization of a Permanent Magnet Motor for an Electric Vehicle. *Tehnički vjesnik, 30*(2), 538-544. https://doi.org/10.17559/TV-20220815140808
[5] Mi, C. G., Hai, Y., Wu, F. Z., Luo, L., Chen, Z. J., Fan, Y. H., & Kang, D. (2023). Fuzzy Multi-Objectives Topology Optimization of Slider Pallet in the Picking Machine of Camellia Fruit. *Tehnički vjesnik, 30*(5), 1627-1634. https://doi.org/10.17559/TV-20230111000218
[6] Fang, J., Gao, Y., Sun, G., & Li, Q. (2013). Multiobjective reliability-based optimization for design of a vehicle door.

Finite Elements in Analysis and Design, 67, 13-21. https://doi.org/10.1016/j.finel.2012.11.007
[7] Yang, M., Zhang, D., Cheng, C., & Han, X. (2021). Reliability-based design optimization for RV reducer with experimental constraint. *Structural and Multidisciplinary Optimization, 63*, 2047-2064. https://doi.org/10.1007/s00158-020-02781-3
[8] Luo, Z., Chen, L. P., Yang, J., Zhang, Y. Q., & Abdel-Malek, K. (2006). Fuzzy tolerance multilevel approach for structural topology optimization. *Computers & structures, 84*(3-4), 127-140. https://doi.org/10.1016/j.compstruc.2005.10.001
[9] Sleesongsom, S. & Bureerat, S. (2020). Multi-objective reliability-based topology optimization of structures using a fuzzy set model. *Journal of Mechanical Science and Technology, 34*, 3973-3980. https://doi.org/10.1007/s12206-020-2207-8
[10] Sun, H. Z., Lei, Z. B., Huang, Y. P., & Yu, J. H. (2020). Multi-objective robust design of new rotate barrel based on satisfaction function. *Tehnički vjesnik, 27*(2), 558-566. https://doi.org/10.17559/TV-20190712135459
[11] Tang, J. C., Jiang, C., Long, X. Y., Zhang, Z., & Liu, H. B. (2019). An interval robust optimization method for uncertain structures. *Chinese Science: Technological Science, 49*(7), 787-802. https://doi.org/10.1360/SST-2019-0052
[12] Li, Z. X., Yang, G. L., Xu, F. J., & Wang, L. Q. (2021). Interval uncertain optimization for damping fluctuation of a segmented electromagnetic buffer under intensive impact load. *Defence Technology, 17*(3), 884-897. https://doi.org/10.1016/j.dt.2020.05.018
[13] Tang, J., Li, X., Fu, C., Liu, H., Cao, L., Mi, C., & Yao, Q. (2024). A possibility-based solution framework for interval uncertainty-based design optimization. *Applied Mathematical Modelling, 125*, 649-667. https://doi.org/10.1016/j.apm.2023.09.010
[14] Ma, Y. S. (2021). *Finite element analysis and structural optimization design of integrated motor-reducer housing*. Shandong University of Technology.
[15] Yan, M. L. (2014). *Research on lightweighting of specialized gearboxes based on topology optimization methods*. Chongqing University of Technology.
[16] Ling, Y. L. & Wei, Z. (2013). Introduction of SolideWorks function in mechanical field and development prospect. *Talent, 2013*(14), 313.
[17] Hu, X. (2024). CAE software operation small encyclopedia (68). *Computer Aided Engineering, 33*(04), 7778.
[18] Mi, C. G. (2014). *Research on fatigue reliability of mining dump truck frame based on strain energy method*. Hunan University.
[19] Wang, H. G. (2016). *Static and dynamic characteristic analysis and optimization design of heavy truck frame*. Chongqing Jiaotong University.
[20] Sun, Z. (2014). *Lightweight design of automotive parts based on multi-objective topology optimization*. Huazhong University of Science and Technology.
[21] Jiang, C., Han, X., Guan, F. J., & Li, Y. H. (2007). An uncertain structural optimization method based on nonlinear interval number programming and interval analysis method. *Engineering Structures, 29*(11), 3168-3177. https://doi.org/10.1016/j.engstruct.2007.01.020
[22] Li, F. Y. & Li, G. Y. (2010). Interval-based uncertain multi-objective optimization design of vehicle crashworthiness. *Computers, Materials & Continua (CMC), 15*(3), 199.
[23] Li, W. T. (2020). *Research on fuzzy fatigue reliability of electric wheel dump truck A-frame considering multi-source uncertainty*. Hunan University of Technology.
[24] Zhang, S. (2018). *Characteristic analysis and optimization of mining dump truck vibration damping system based on interval method*. Hunan University.
[25] Xiao, X. W. (2021). *Research on the multi-objective optimal design of electric wheel dump truck frame based on interval method*. Hunan University of Technology.

Contact information

Di KANG
Hunan Academy of forestry,
No. 658 Shaoshan South Road, Changsha, Hunan Province, China
E-mail: 13838@hut.edu.cn

Longsheng CHEN
Hunan Academy of forestry,
No. 658 Shaoshan South Road, Changsha, Hunan Province, China

Shaofeng PENG
Hunan Academy of forestry,
No. 658 Shaoshan South Road, Changsha, Hunan Province, China

Wangyuan LI
Hunan Shennong National Oil Ecological Agriculture Development Co.,
Shennong National Oil Industrial Park,
No. 1998 Shennong North Road, Qiling Neighbourhood Committee,
Sanjia Office, Leiyang City, China

Delin WU
Anhui Agricultural University,
No. 130 West Changjiang Road, Hefei City, Anhui Province, China

Yang HAI
Department of Mechanical Engineering, Hunan University of Technology,
No. 88 West of Taishan Road, Zhuzhou City, China
E-mail: haiyang_hut@126.com

Chengji MI
(Corresponding Author)
Department of Mechanical Engineering, Hunan University of Technology,
No. 88 West of Taishan Road, Zhuzhou City, China
E-mail: michengji_86@126.com